

# Numerical Modeling of Earthquake Dynamic Rupture: Requirements for Realistic Modeling

Eiichi Fukuyama\*

National Research Institute for Earth Science and Disaster Prevention

## Abstract

I propose a strategy to make a numerical computation applicable to the realistic modeling of an earthquake dynamic rupture process. To do this, it is important to introduce any observables into the simulation as initial and boundary conditions. As an initial condition, distribution of total stress before the dynamic rupture, and as boundary conditions, fault constitutive relation and geometry of the fault are necessary. The initial stress distribution would be obtained by both *in-situ* measurements of stress and stress tensor inversions of earthquake focal mechanisms. Constitutive parameters could be obtained by near fault observations of seismic waves. Precise fault geometry can be obtained by an accurate relocation of seismicity as well as geological survey. Realistic simulations of a dynamic rupture of an earthquake can only be done by integrating the above observations.

**Key words:** numerical modeling, earthquake dynamic rupture, drilling project

## Introduction

Recent rapid progress in computations for the dynamic modeling of earthquake faulting enables us to model a realistic earthquake rupture based on boundary integral equation method (Fukuyama and Madariaga, 1998; Aochi *et al.*, 2000 a), finite difference method (Olsen *et al.*, 1997; Madariaga *et al.*, 1998), finite element method (Oglesby *et al.*, 1998), or distinct element method (Mora and Place, 1998; Dalguer *et al.*, 2001).

When modeling earthquake dynamic rupture using the above techniques, there is a lot of freedom in simulating the dynamic rupture. Thus, detailed information on both initial and boundary conditions of the fault is required. Initial condition is the initial stress field along the fault and boundary conditions are fault geometry and constitutive parameters of the fault such as slip weakening distance and fault strength. On the other hand, there are a lot of observations such as seismic waveform analysis (e.g. Ide and Takeo, 1997) *in-situ* measurements inside a drilling borehole (e.g. Tsukahara *et al.*, 1996), laboratory experiments (e.g. Malone and Kilgore, 1993; Ohnaka and Shen, 1999), and core analyses (e.g. Tanaka *et al.*,

2001ab), which might constrain more precisely the initial and boundary conditions of a dynamic rupture model of an earthquake. Thus, it becomes possible to incorporate these results into a numerical model.

When modeling the earthquake generation process, scales in space and time should be taken into account. There are three stages in an earthquake cycle: (1) steady state stage where healing and stress buildup are underway, (2) nucleation stage, when quasi-static deformation is taking place for the main rupture of earthquake, and (3) dynamic rupture stage, in which the earthquake occurs with strong seismic wave radiation. In the steady-state stage, long time-scale behavior should be treated, and thus the rheological property of the crust and tectonic loading process become important (Hashimoto and Matsu'ura, 2002). To render an overall behavior of the system, large-scale modeling in space and time is required. At the earthquake nucleation stage (i.e. during quasi-static process), a shorter time scale than in steady-state modeling, but with a finer structure becomes important to describe this process (Lapusta *et al.*, 2000). In dynamic rupture modeling, which I

---

\* e-mail: fuku@bosai.go.jp, (3-1 Tennodai, Tsukuba, Ibaraki, 305-0006, Japan)

discuss, short time scale behavior should be described accurately, while rheological properties can be neglected (Okubo, 1989; Cocco and Bizzarri, 2002).

In this paper, I compile information which is helpful for numerical modeling to show the strategy to construct a model of the earthquake dynamic rupture process. This strategy might also be useful as a physical basis for strong ground motion predictions in which the distribution of asperities becomes critical information.

### Important Parameters

Dynamic rupture propagation is basically controlled by the boundary integral equation shown in Eq. 1, which is derived from the equation of motion with stress continuity on the fault.

$$\tau(x, t) = -\frac{\mu}{2\beta}\Delta\dot{u}(x, t) + \iint_S \Delta\dot{u}(\xi, \tau)K(x-\xi, t-\tau)dxdt \quad (1)$$

where  $\tau$  is shear stress,  $\Delta\dot{u}$  is sliprate on the fault,  $\mu$  and  $\beta$  are rigidity and shear wave velocity, respectively, and  $S$  is the area of the fault.  $K$  is the integration kernel, which is rigorously shown by Fukuyama and Madariaga (1998) for a planar crack and Tada *et al.* (2000) for a curved crack. It should be emphasized that this equation is independent of the constitutive relation, because it is derived only from the continuity and the symmetry/asymmetry of stress and displacement across the fault. To model an earthquake rupture process accurately, the initial and boundary conditions are crucial. The boundary condition is the geometry of the fault and the constitutive relation on the fault. The initial condition is the stress field on and around the fault before the dynamic rupture.

Thus, I consider three important inputs here for modeling the dynamic ruptures of earthquakes: (1) fault geometry,  $S$ , (2) constitutive relation,  $\tau(x, t) = F(\Delta u(x, t))$  and (3) initial stress field,  $\tau(x, 0)$ . When considering the dynamic rupture process, the slip weakening constitutive relation is sufficient (Okubo 1989; Cocco and Bizzarri, 2002). Thus, I use the slip-weakening law as a constitutive relation.

In the following sections, each condition is discussed in detail.

### Fault Geometry

An earthquake fault can be modeled by a single planar surface as a zero-th order approximation. However, if we look in more detail, an earthquake fault surface is not planar. There are many jogs, kinks and branches. These complicated geometries may affect to the simulation of earthquake dynamic rupture process.

Harris and Day (1993, 1999) and Kase and Kuge (1998) investigated fault interactions during the dynamic rupture for parallel or perpendicular fault segments. Aochi *et al.* (2000 a b) demonstrated that fault kink and fault branch have a significant effect on dynamic rupture propagation in a more general situation. From these results, fault geometry produces stress heterogeneity on the fault, which causes a variety of dynamic rupture propagation.

Aochi and Fukuyama (2002) succeeded in modeling the dynamic rupture of the 1992 Landers, California, earthquake based on fault geometry obtained by geological survey (Hart *et al.*, 1993) with very simple assumptions for stress field and constitutive relations. This indicates that the precise geometry of faults enables us to model an earthquake dynamic rupture under a physically reasonable situation.

Moreover, even when no surface trace appeared after an earthquake, a precise fault geometry can be obtained if aftershocks are relocated with enough precision. Fukuyama *et al.* (2003 a) analyzed the aftershock sequence of the 2000 western Tottori earthquake using the double difference (DD) method (Waldhauser and Ellsworth, 2000) and obtained a very clear image of the fault system (Fig. 1), which is consistent with the moment tensor solutions of aftershocks. Sagiya *et al.* (2002) used this fault model for the analysis of geodetic data, and discussed a post-slip deformation. Thus, even if there is no fault breakout, precise relocations of earthquakes give us important information for dynamic rupture modeling.

### Initial Stress Field

It is very difficult to measure the distribution of total stress along a fault because the only possible measurement we can take is strain. Stress can only be estimated through the strain distribution.

In order to get the total stress distribution along the fault, I take the following two steps: (1) relative stress field is estimated by a stress tensor inversion

a) Relocated hypocenters and strike directions    b) Fault model based on relocated hypocenters and aftershock moment tensors

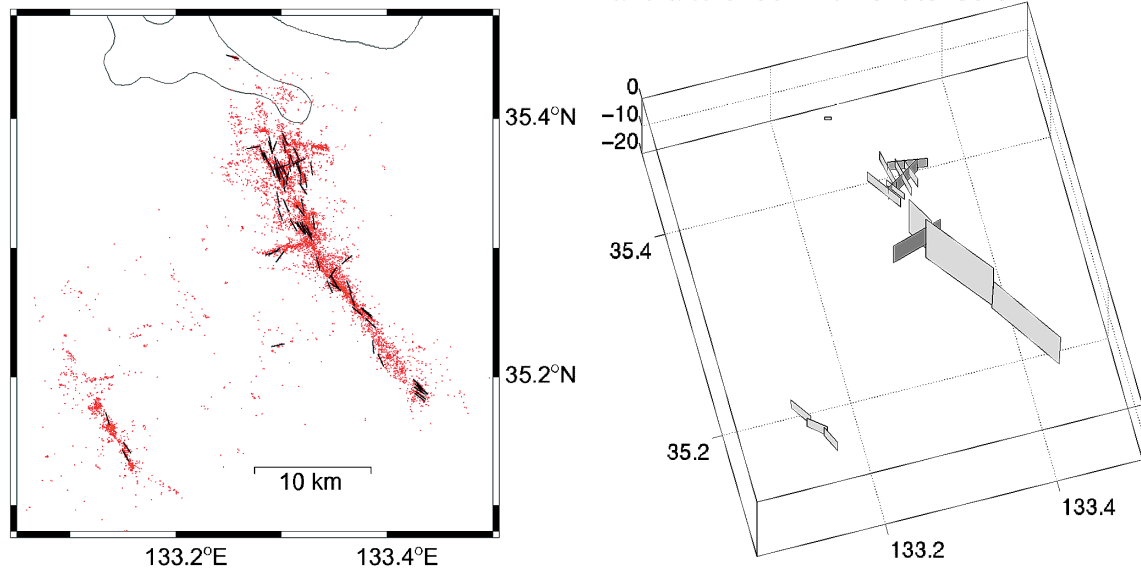


Fig. 1. a) Relocated hypocenters of the 2000 western Tottori aftershocks are plotted as red points. Hypocenters are computed by the double difference method during the period from Oct. 06, 2000 to Nov. 17, 2000; in total, 8516 events are plotted. Strike directions of 77 medium-sized aftershocks ( $M_w \geq 3.5$ ) are also plotted as black bars, which are obtained by the moment tensor inversion of broadband seismograms in regional distance. (after Fukuyama *et al.*, 2003 a) b) Fault models derived by both relocated hypocenters and focal mechanisms of aftershocks. (after Fukuyama *et al.*, 2003 a)

using focal mechanisms of earthquakes. Then, (2) *in-situ* measurements at the bottom of a borehole enables us to estimate total stress, which can calibrate the relative stress field measured in step (1).

Fukuyama *et al.* (2003 a) estimated the relative stress field after the 2000 western Tottori earthquake using aftershock moment tensor solutions of regional waveforms (Fig. 2). They provided a very stable relative stress field. Unfortunately, since there were no *in-situ* stress measurements for the western Tottori aftershock region, the total stress field cannot be obtained yet.

### Constitutive Parameters

Two constitutive relations have been proposed: rate- and state-dependent friction law (e.g. Dieterich, 1979) and slip-weakening friction law (e.g. Matsu'ura, *et al.*, 1992). During the dynamic rupture of an earthquake, the slip weakening property of friction is considered to be dominant (Okubo, 1989; Cocco and Bizzarri, 2002). Thus the problem becomes how to estimate slip weakening distance, breakdown stress drop and shape of slip weakening curve from observations.

Ide and Takeo (1997) proposed a method to estimate slip-weakening distance on a fault using spatio-temporal sliprate function estimated by waveform inversion. And Guatteri and Spudich (2000) showed the limitation of the resolution due to the trade-off between slip-weakening distance and breakdown stress drop. They insisted that stable estimates might be fracture energy, which is proportional to the product of the two parameters above.

Recently, Mikumo *et al.* (2003) proposed a simple method to estimate slip weakening distance from near fault waveforms. In their estimation, they assume that stress break-down time is very close to the peak slip velocity time (Fig. 3 a). This assumption is valid provided the rupture velocity does not change abruptly and slip weakening curve has a rather sharp change in its gradient at the stress break-down time (Fukuyama *et al.*, 2003 b). This method enables us to separate slip weakening distance and fracture energy.

During the 2000 western Tottori earthquake, two near fault strong motion records were obtained at GSH and TTRH02 (Fig. 3 b). Their ground displacements and velocities along the fault strike direction

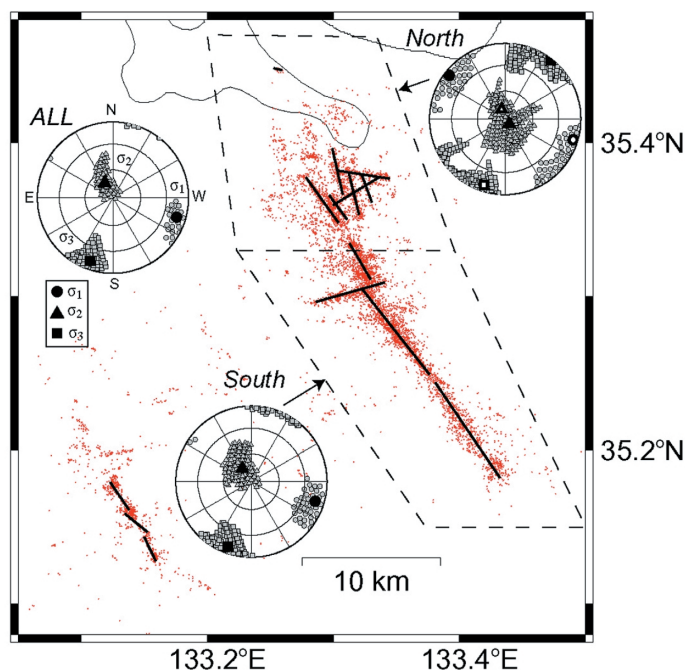


Fig. 2. The results of stress tensor inversion for three different datasets of the 2000 western Tottori aftershock sequence. “ALL” depicts the result for the entire data; “North” and “South” show the results for the surrounded regions by broken lines, respectively. Closed circles, triangles, and squares indicate maximum ( $\sigma_1$ ), intermediate ( $\sigma_2$ ), and minimum ( $\sigma_3$ ) stress directions, respectively. Small gray symbols show the 95% confidence region of each stress direction estimate. Open symbols in the “North” result stands for the alternative result, which is suitable for the large  $R$  ( $=(\sigma_1 - \sigma_2)/(\sigma_1 - \sigma_3)$ ) environment. Solid lines on the hypocenter distribution correspond to the fault model shown in Fig. 1 b. (After Fukuyama *et al.*, 2003 a).

are shown in Fig. 3 b. Although these stations are very close to the fault, they are not located exactly on the fault and the waveforms could not be considered as slip functions. Some numerical simulations of dynamic rupture are required to calibrate the observed near-fault seismograms for the estimation of slip function on the fault.

The drilling project penetrating across the fault gives us the possibility of observing on-fault motion using a seismometer, which corresponds to the slip function itself. If a seismometer is installed in the borehole near the fault plane and an earthquake occurs (of course, such situation is considered to be very rare), such seismograms provide us with tremendous information on fault constitutive relations.

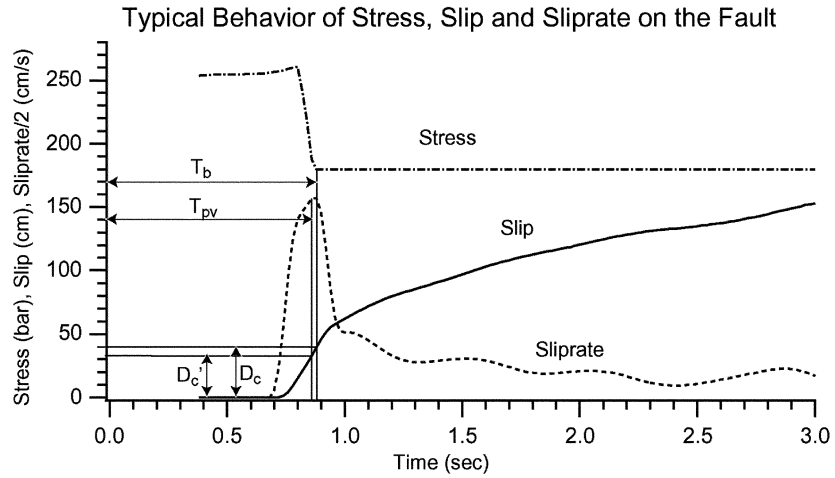
#### Integration of Borehole Experiments and Numerical Modeling

It is important to include additional information obtained by independent surveys in numerical mod-

eling. Downhole measurements at the bottom of a borehole might give us substantial information. The total stress field can only be obtained from direct measurements on and around the fault at depth. Frictional properties can also be obtained through an analysis of core samples obtained by drilling. Thus, an integration between *in-situ* experiments during borehole drilling with related laboratory experiments and numerical modelings are required under well-organized conditions.

There are several discussions about the thickness of the fault. A trapped wave survey provided us with a fault thickness of about 100 m (e.g. Li *et al.*, 1994, Ito and Kuwahara, 1996). On the other hand, a fault core analysis suggests that the slip zone is of very limited thickness ( $\sim cm$ ) (e.g. Tanaka *et al.*, 2001a, Kobayashi *et al.*, 2001, Tomita *et al.*, 2002, Omura *et al.*, 2002) (Fig. 4). It might be important to discriminate these observations to obtain a suitable modeling for numerical simulation.

### (a) Schematic Explanation



### (b) Example of Observations

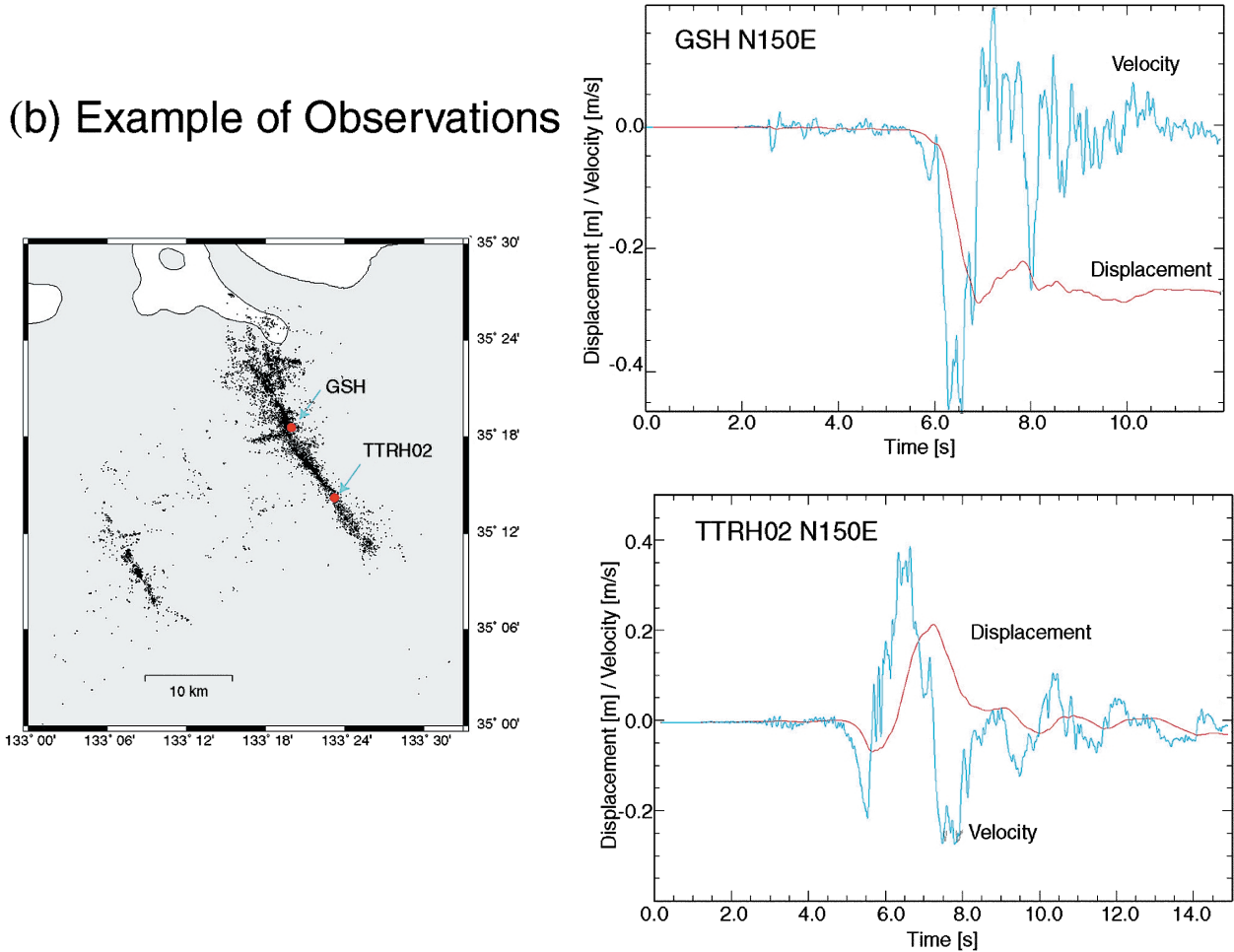


Fig. 3. (a) Schematic illustration of the  $D_c$  estimation method.  $T_b$  and  $D_c$  correspond to the breakdown stress time and slip weakening distance, respectively.  $T_{pv}$  is the peak sliprate time and  $D'_c$  is the slip at  $T_{pv}$ . If  $T_{pv}$  is close to  $T_b$ ,  $D'_c$  becomes a good estimate for  $D_c$  (after Mikumo *et al.*, 2003). (b) An example of field observations during the 2000 western Tottori earthquake. There are two stations, which are located above the fault plane (see left panel). The fault parallel ground motions observed at these two stations are also shown in the right panels.

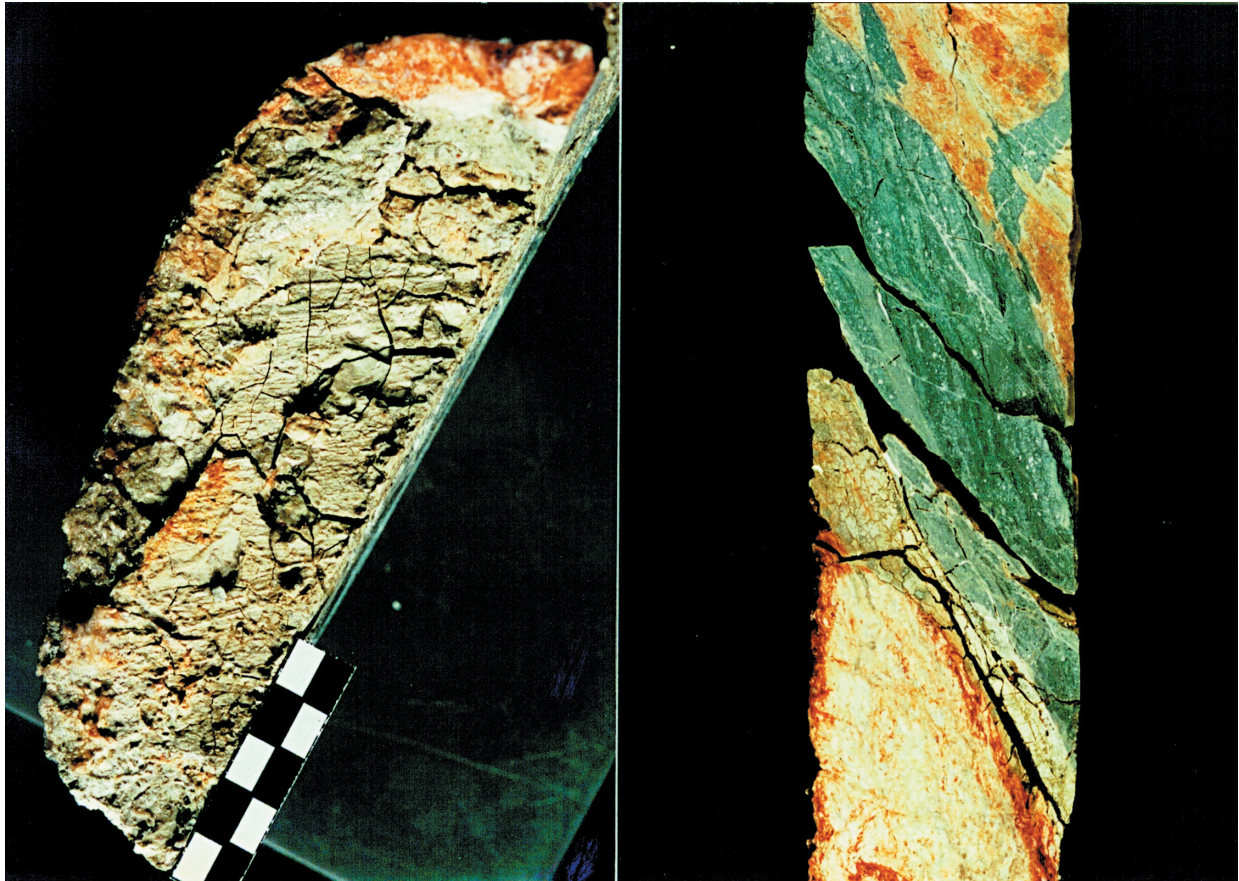


Fig. 4. Photographs of the NIED Nojima Hirabayashi cores at the depth of 1140 m. (a) Left panel shows the fault surface, which slipped during the 1995 Kobe earthquake. Several slickensides can be recognized on the slickenside. (after Kobayashi *et al.*, 2002). (b) Right panel shows the cores across the fault along the depth. (after Omura *et al.*, 2002).

The major problem in drilling experiments is that the measurements are done only at a point. Thus, a method to extrapolate the observation in the borehole should be developed. Because the depth is strongly constrained by the technology available, as well as budget, the problem also occurs of how to extrapolate a result at a shallow depth to that at a seismogenic depth. Thus, in order to include the drilling result in the numerical modeling of earthquake dynamics, these extrapolation problems should be considered very carefully.

### Conclusion

I proposed a strategy to make a numerical computation that is applicable to the realistic modeling of a dynamic rupture process. To do this, it is important to introduce available observations into the simulation. Initial stress distribution will be obtained by both *in-situ* measurement of stress and stress tensor inversion of earthquake focal mecha-

nisms. Constitutive parameters could be obtained by near fault observations of seismic waves. Precise fault geometry can be obtained from the accurate relocations of seismicity. Realistic simulations can only be done using these observations.

### Acknowledgments

Critical readings by Prof. Kikuchi and an anonymous reviewer helped improve the manuscript. This work was supported by the NIED project entitled “Research on Earthquake Source Mechanisms.”

### References

- Aochi, H., E. Fukuyama and M. Matsu'ura, 2000 a, Spontaneous rupture propagation on a non-planar fault in 3-D elastic medium, *PAGEOPH*, **157**, 2003–2027.
- Aochi, H., E. Fukuyama and M. Matsu'ura, 2000 b, Selectivity of spontaneous rupture propagation on a branched fault. *Geophys. Res. Lett.*, **27**, 3635–3638.
- Aochi, H. and E. Fukuyama, 2002, 3D non-planar simulation of the 1992 Landers earthquake, *J. Geophys. Res.*, **107** (B2), 10.1029/2000JB000061.

- Aochi, H., R. Madariaga and E. Fukuyama, 2002, Effect of normal stress during rupture propagation along non-planar faults, *J. Geophys. Res.*, **107** (B2), 10.1029/2001JB000500.
- Cocco, M. and A. Bizzarri, 2002, On the slip-weakening behavior of rate- and state- dependent constitutive laws, *Geophys. Res. Lett.*, **29**, 1–4.
- Dalguer, L. A., K. Irikura, J. D. Riera and H. C. Chiu, 2001, Fault dynamic rupture simulation of the hypocenter area of the thrust fault of the 1999 Chi-Chi (Taiwan) earthquake, *Geophys. Res. Lett.*, **28**, 1327–1320.
- Dieterich, J. H., 1979, Modeling of rock friction I. Experimental results and constitutive equations, *J. Geophys. Res.*, **84**, 2161–2168.
- Fukuyama, E. and R. Madariaga, 1998, Rupture dynamics of a planar fault in a 3D Elastic medium: rate- and slip-weakening friction, *Bull. Seism. Soc. Amer.*, **88**, 1–17.
- Fukuyama, E. and R. Madariaga, 2000, Dynamic propagation and interaction of a rupture front on a planar fault, *PAGEOPH*, **157**, 1959–1979.
- Fukuyama, E., W. L. Ellsworth, F. Waldhauser and A. Kubo, 2003a, Detailed fault structure of the 2000 western Tottori, Japan, earthquake sequence, *Bull. Seism. Soc. Amer.*, **93**, 1468–1478.
- Fukuyama, E., T. Mikumo and K. B. Olsen, 2003b, Estimation of critical slip-weakening distance: Theoretical background, *Bull. Seism. Soc. Amer.*, **93**, 1835–1840.
- Guatteri, M. and P. Spudich, 2000, What can strong-motion data tell us about slip-weakening fault-friction laws?, *Bull. Seism. Soc. Amer.*, **90**, 98–116.
- Harris, R. A. and S. M. Day, 1993, Dynamics of fault interaction: parallel strike-slip faults, *J. Geophys. Res.*, **98**, 4461–4472.
- Harris, R. A. and S. M. Day, 1999, Dynamic 3D simulations of earthquakes on en echelon faults, *Geophys. Res. Lett.*, **26**, 2089–2092.
- Hart, E. W., W. A. Bryant and J. A. Treiman, 1993, Surface faulting associated with the June 1992 Landers, California, *Calif. Geol.*, **46**, 10–16.
- Hashimoto, C. and M. Matsu'ura, 2002, 3-D simulation of earthquake generation cycle at transcurrent plate boundaries, *PAGEOPH*, **159**, 2175–2199.
- Ide, S. and M. Takeo, 1997, Determination of constitutive relations of fault slip based on seismic wave analysis, *J. Geophys. Res.*, **102**, 27379–27391.
- Ito, H. and Y. Kuwahara, 1996, Trapped waves along the Nojima fault from the aftershock of Kobe earthquake, 1995, *Proc. VIII<sup>th</sup> Int. Symp. Obs. Continent. Crust Trough Drilling*, 399–402.
- Kase, Y. K. Kuge, 1998, Numerical simulation of spontaneous rupture process on two non-coplanar faults: the effect of geometry on fault interaction, *Geophys. J. Int.*, **135**, 911–922.
- Kobayashi, K., S. Hirano, T. Arai, R. Ikeda, K. Omura, H. Sano, T. Sawaguchi, H. Tanaka, T. Tomita, N. Tomida, T. Matsuda and A. Yamazaki, 2001, Distribution of fault rocks in the fracture zone of the Nojima fault at a depth of 1140 m: observations from the Hirabayashi NIED drill core, *The Island Arc*, **10**, 411–421.
- Lapusta, N., J. R. Rice, Y. Ben-Zion and G. Zheng, 2000, Elastodynamic analysis for slow tectonic loading with spontaneous rupture episodes on faults with rate- and state-dependent friction, *J. Geophys. Res.*, **105**, 23765–23789.
- Li, Y.-G., K. Aki, D. Adams and A. Hasemi, 1994, Seismic guided waves trapped in the fault zone of the Landers, California, earthquake of 1992, *J. Geophys. Res.*, **99**, 11705–11722.
- Madariaga, R., K. B. Olsen and R. J. Archuleta, 1998, Modeling dynamic rupture in a 3-D earthquake fault model, *Bull. Seis. Soc. Amer.*, **88**, 1182–1197.
- Marone, C. and B. Kilgore, 1993, Scaling of the critical slip distance for seismic faulting with shear strain in fault zones, *Nature*, **362**, 618–621.
- Matsu'ura, M., H. Kataoka and B. Shibazaki, 1992, Slip-dependent friction law and nucleation process in earthquake rupture, *Tectonophysics*, **211**, 135–148.
- Mikumo, T., K. B. Olsen, E. Fukuyama and Y. Yagi, 2003, Stress-breakdown time and slip-weakening distance inferred from slip-velocity function on earthquake faults, *Bull. Seism. Soc. Amer.*, **93**, 264–282.
- Mora, P. and D. Place, 1998, Numerical simulation of earthquake faults with gouge: towards a comprehensive explanation for the heat flow paradox, *J. Geophys. Res.*, **103**, 21067–21089.
- Oglesby, D. D., R. J. Archuleta and S. B. Nielsen, 1998, Earthquakes on dipping faults: the effects of broken symmetry, *Science*, **280**, 1055–1059.
- Ohnaka, M. and L.-F. Shen, 1999, Scaling of the shear rupture process from nucleation to dynamic propagation: implication of geometric irregularity of the rupturing surfaces, *J. Geophys. Res.*, **104**, 817–844.
- Okubo, P. G., 1989, Dynamic rupture modeling with laboratory-derived constitutive relations *J. Geophys. Res.*, **94**, 12321–12335.
- Olsen, K. B., R. Madariaga and R. J. Archuleta, 1997, Three-dimensional dynamic simulation of the 1992 Landers earthquake, *Science*, **278**, 834–838.
- Omura, K., R. Ikeda, T. Matsuda, T. Arai, K. Kobayashi, K. Shimada, H. Tanaka, T. Tomita and S. Hirano, 2002, Photographs of NIED Nojima fault drilling cores at Hirabayashi borehole, *Tech. Note Nat'l Res. Inst. Earth Sci. Disas. Prev.*, **229**, 1–7.
- Sagiya, T., T. Nishimura, Y. Hatanaka, E. Fukuyama and W. L. Ellsworth, 2002, Crustal movements associated with the 2000 western Tottori earthquake and its fault models, *Zisin Ser. 2*, **54**, 523–534 (in Japanese with English abstract).
- Tada, T., E. Fukuyama and R. Madariaga, 2000, Non-hyper-singular boundary integral equations for 3-D non-planar crack dynamics, *Comp. Mech.*, **25**, 613–626.
- Tanaka, H., T. Matsuda, K. Omura, R. Ikeda, K. Kobayashi, K. Shimada, T. Arai, T. Tomita and S. Hirano, 2001a, Complete fault rock distribution analysis along the Hirabayashi NIED core penetrating the Nojima fault at 1,140 depth, Awaji island, southwest Japan, *Rep. Nat'l Res. Inst. Earth Sci. Disas. Prev.*, **61**, 195–221.
- Tanaka, H., S. Hinoki, K. Kosaka, A. Lin, K. Takemura, A. Murata and T. Miyata, 2001b, Deformation mechanisms and fluid behavior in a shallow, brittle fault zone during coseismic and interseismic periods: results from drill core penetrating the Nojima fault, Japan, *The Is-*

- land Arc*, **10**, 381–391.
- Tomita, T., T. Ohtani, N. Shigematsu, H. Tanaka, K. Fujimoto, Y. Kobayashi, Y. Miyashita and K. Omura, 2002, Development of the Hatagawa fault zone clarified by geological and geochronological studies, *Earth Planets Space*, **54**, 1095–1102.
- Tsukahara, H., R. Ikeda and K. Omura, 1996, In-situ stress measurement in an earthquake focal area, *Tectonophys.*, **262**, 281–290.
- Waldhauser, F. and W.L. Ellsworth, 2000, A double-difference earthquake location algorithm: Method and application to the northern Hayward fault, California, *Bull. Seism. Soc. Amer.*, **90**, 1353–1368.
- (Received February 21, 2003)  
(Accepted July 15, 2003)